Nonlinear optical response due to resonant enhancement of the internal field with particular spatial distribution

Hajime Ishihara*
Precursory Research for Embryonic Science and Technology, Research Development Corporation of Japan, c/o Advanced Device Technology Department, Semiconductor Research Laboratory, Mitsubishi Electric Corporation, 1-1, Tsukaguchi Honmachi 8-Chome, Amagasaki, Hyogo 661, Japan

Kikuo Cho
Department of Material Physics, Faculty of Engineering Science, Osaka University, Toyonaka, Osaka 560, Japan
(Received 31 March 1995; revised manuscript received 15 November 1995)

Peculiar properties of nonlinear response, due to a resonant enhancement of internal field are predicted for the mesoscopic systems by means of a nonlocal theory of nonlinear response. In this theory, self-consistent motions of the internal field and the induced polarization, which are related nonlocally with each other, are determined by solving the equation system of Schrödinger and Maxwell's equations. A study with a model of ultrathin films consisting of one-dimensional Frenkel excitons has clarified the following points: As a result of a self-consistent motion with the induced polarization, the internal field with a characteristic spatial distribution associated with each quantized exciton state is enhanced at a particular resonant energy including a radiative correction that depends on system size. This resonant enhancement of the internal field greatly strengthens the nonlinear signal of a particular third-order process, leading to a remarkable size and energy dependence of the nonlinear response. This effect is explicitly demonstrated for a particular type of pump-probe spectroscopy. [S0163-1829(96)00723-0]

I. INTRODUCTION

Recently, the requirement of highly efficient optical devices in the field of optoelectronics accelerates the investigations of nonlinear optical materials. Especially, ultrasmall or low dimensional systems (mesoscopic systems) such as fine particles, quantum wells (wires, dots), and thin films, which confine electronic systems, and have become important objects of the research of nonlinear optical phenomena. At the same time, through the detailed study of these systems, new fundamental aspects of the optical response of confined electronic systems have also come to our attention.

One of the main reasons for the great attention to the confined electronic systems is that these materials show a remarkable size dependence in nonlinear response. For the expectation of large nonlinearity, a lot of works have given arguments on the size-dependent nonlinearity of confined electronic systems, and most of them attribute this phenomenon to the size dependence of the third-order nonlinear susceptibility $\chi^{(3)}$.[1–6] Some discussions are based on the idea of the size enhancement of oscillator strength,[1–4] namely, the oscillator strength increases in proportion to the system size as long as the wave function of exciton is coherent in the whole sample, and this brings about size-linear enhancement of $\chi^{(3)}$. This argument is valid in the limited size range where a long-wavelength approximation (LWA) is valid. However, it does not give a consistent description when LWA is not applicable, because the concept of the oscillator strength is based on LWA. It should also be noted that the separation of nonlinear polarization into ''position-independent'' susceptibility and field amplitudes, which is the background of the size enhancement of $\chi^{(3)}$, is allowed only in a LWA.

As we discussed in the previous papers,[7–11] the basic concept for the comprehensive understanding of the size dependence of optical properties is ''nonlocal response.'' In general, the density of induced dipole moment at some point of a matter is determined by the electric field not only at that point, but also at other points, because of the finite extension of the wave functions of relevant states. This should be described as the relationship between the internal field and induced dipole density in the nonlocal form, namely, one quantity is described as a functional of another quantity.[10] In this way, the spatial distribution of the internal field is determined consistently with that of induced polarization. Thus, for a resonant light, the spatial variation of the internal field becomes comparable to that of induced polarization, and in a mesoscopic system where the polarization wave is coherent in the whole sample, the magnitude and the spatial distribution of the internal field are resonantly dependent on the ''size, shape, and internal structure'' of the sample.[8,10,11] Since this effect of the internal field should strongly affect the resonant nonlinear response, the consideration of nonlocality beyond the arguments of size enhancement of $\chi^{(3)}$ is absolutely necessary for the consistent understanding of nonlinear response. This is essential for the description of the size dependence from microscopic to macroscopic range, but even in the LWA regime it can be very important as mentioned below.

In Ref. 9, we developed a nonlocal theory of nonlinear response, where the site represented linear and nonlinear susceptibilities are calculated for a model systems of an ultrathin film consisting of one-dimensional chains confining Frenkel excitons and then, the Maxwell equations containing these source terms are solved. Since the energy transfer and damping, which determines the extent of the coherence of electronic systems, are explicitly taken into account, and

since the self-consistent motions of the field and induced polarization are determined in this method, the effect of ''size, shape, and internal structure'' dependence of both susceptibility and the internal field are automatically incorporated in the final result. From a fully nonlocal calculation in a small size region (up to 20 molecule layers of CuCl thin film), we obtained a clear indication of nonlocality and the size dependence of internal field in the response spectra, even though the system size belongs to the LWA region, where the position dependence of the internal field should be negligible.

On the other hand, in Refs. 8,10, we discussed peculiar resonant behavior of the internal field that appears in the size region where the position dependence of the internal field is noticeable. Namely, the component with particular spatial pattern of the internal field shows resonant size enhancement. In these papers, we saw this effect in the case that beam energy was fixed at the lowest excitonic level, where the component of the internal field relevant to the second excitonic level is resonantly enhanced even when the beam energy is tuned to the lowest level. Further, in Ref. 11, we studied the nonlinear response caused by the enhancement of the internal field, extending the size range of the calculation for the same model as in Ref. 9, and it has been clarified, for the case of pump-probe spectroscopy, that a certain nonlinear signal is remarkably strengthened because of the simultaneous resonances of the internal field in energy and size. We called this effect ''Nonlocality-induced double resonance in energy and size (NIDORES).''

In the above papers, we focused on a specific aspect of the problem, namely, we discussed the size dependence of the internal field and the nonlinear signal keeping the pump beam energy at the particular excitonic (material) level. This effect, however, appears in different ways according to the choice of a fixed parameter, since the signal intensity is a function of pump and probe beam frequencies and of sample size (N). Therefore, in this paper, we study the resonant enhancement of the internal field and resulting nonlinear response in more general way, changing a fixed parameter.

The rest of this paper is organized as follows: Before the calculation of the nonlinear response, we supplement the arguments on the resonant enhancement of internal field in an ultrathin film that were given in Refs. 8,10. Then we proceed to a nonlinear response, in Sec. III, to see the effect of the strong nonlocality on the nonlinear properties of mesoscopic systems, where a pump-probe spectroscopy is handled. In Sec. IV, we give a detailed analysis of the structures in the calculated nonlinear spectra, assigning the peak structures to specific transitions. The discussions and summary are given in the succeeding sections.

II. INTERNAL FIELD IN AN ULTRATHIN FILM

In this section, we consider the magnitude and spatial variation of the internal field of resonant light in an ultrathin semiconductor film. A theoretical description of linear response in a film has been done by various groups,[12–18] and it is now well established that, for a thickness much larger than exciton Bohr radius, only the size quantization of center-of-mass (CM) motion needs to be considered. In order to make a smooth continuation to the model for nonlinear processes later, we will handle the problem in terms of a discrete lattice model, which is exactly the same as those in Refs. 8 and 11. Namely, we consider the film consisting of N layers in which the motion of Frenkel excitons parallel to the axis of the film are confined. We assume the amplitude of exciton is zero on the imaginary 0th and $(N+1)$th layers, and neglect the possible distortion of exciton wave functions near the film surfaces. This model gives essentially the same result as that of continuum model based on Wannier excitons with the properly chosen parameter values for the transfer energy and the transition dipole moment per unit cell.[19] This treatment is useful in the case where exciton Bohr radius is so small that the consideration of the distortion of wave functions near the surfaces is not necessary. More details of this model are given in Refs. 8,11. By the ABC-free theory, which is the nonlocal theory for the linear response,[16,20] we can obtain the explicit expression of the internal field. The procedure of calculations is almost the same as that in Ref. 16. The main difference is discreteness of the lattice in the present model, in contrast to the continuum model in Ref. 16. The resultant expression of internal field as a function of site j is

$$\mathcal{E}_j=(2\cos q_1-2\cos q_0)\{\overline{\mathcal{E}_1}\sin q_1 j+\overline{\mathcal{E}_2}\sin q_1(N+1-j)\}/\sin q_1(N+1)$$
$$-(2\cos q_2-2\cos q_0)\{\overline{\mathcal{E}_1}\sin q_2 j+\overline{\mathcal{E}_2}\sin q_2(N+1-j)\}/\sin q_2(N+1), \tag{1}$$

where $\overline{\mathcal{E}_1}$ and $\overline{\mathcal{E}_2}$ are arbitrary constants to be determined by the boundary conditions, q_0 is defined as

$$\cos q_0=(\varepsilon_0+2b-\hbar\omega-i\Gamma)/2b, \tag{2}$$

and q_1 and q_2 are the wave numbers of the bulk polaritons that are the roots of the dispersion relation,

$$(2\cos q-2\cos q_b)(2\cos q-2\cos q_0)-B=0. \tag{3}$$

In the above expressions (2) and (3), $b(>0)$ is the nearest layer transfer energy, Γ the phenomenological damping constant of the exciton, and

$$q_b=(\omega/c)\sqrt{\varepsilon_b}, \tag{4}$$

$$B=\frac{\Delta_{\mathrm{LT}}a_0^2\omega^2\varepsilon_b}{bc^2}, \tag{5}$$

where

$$\Delta_{\mathrm{LT}}=\frac{4\pi|M|^2}{a_0^3}, \tag{6}$$

ε_b the background dielectric constant, a_0 the lattice constant, and M the matrix element of the transition dipole moment of the atom. Connecting the internal field with the outer fields by means of Maxwell boundary conditions, we determine the amplitudes of the internal field.

For the study of the spatial structure of the internal field caused by the excitonic resonance, first, we expand $\mathcal{E}_j$, for $1\leqslant j\leqslant N$, in terms of eigenfunctions of translational (CM) motion of excitons in the film, namely,

$$\mathcal{E}_j=\sum_{n=1}^{N}\left(\frac{2}{N+1}\right)^{1/2}\sin\left(\frac{n\pi}{N+1}j\right)F_n. \tag{7}$$

In this expression, n corresponds to the size-quantized wave number (see Ref. 8), and expansion coefficient F_n means the amplitude of the component related with the nth quantized exciton. Throughout the numerical calculations in this section, we choose material parameters of the Z_3 exciton of CuCl that is a typical single-component exciton. The values of parameters are

$$\begin{aligned}&\omega_T=3202.2\ \text{meV},\quad b=57.0\ \text{meV},\\&\frac{4\pi|M|^2}{v_0}=5.7\ \text{meV},\\&\varepsilon_b=5.6,\ \ a_0=5.4\ \text{Å},\end{aligned} \tag{8}$$

where ω_T is the energy of the bottom of the exciton band for $N\rightarrow\infty$, namely, $\omega_T=\varepsilon_0-2b$.

In Fig. 1, we show $|F_n|^2(n=1,2,\text{and }3)$ as a function of beam energy and size N, together with the curves indicating the values of $|F_n|^2$ at the lowest exciton level in each size (the dotted lines on the surface of $|F_n|^2$). In each case of n, we see a specific structure of ridges and valleys. This resonant behavior of the internal field can be understood as another aspect of polariton interference effect, which is well understood for a thin film (for example, see Ref. 21). From these pictures, we know how each component of the internal field is enhanced with the size or energy. If we fix the beam energy, we can see the resonant enhancement of $|F_n|^2$ by size. On the other hand, we find the enhancement of $|F_n|^2$ at the resonant energy of the response field that includes the radiative shift, if we fix the size (N) and change the beam energy. In Ref. 11, we discussed the size dependence of $|F_n|^2$ when the beam energy is tuned to the lowest exciton level, and showed the remarkable resonant enhancement at a certain size (Fig. 2 in Ref. 11). The cross sections along dotted lines are nothing but the curves in Fig. 2 in Ref. 11. The pictures of the resonant structure of each component of the internal field shown here help us to understand the peculiar spectral structure and the size dependence of the resonant nonlinear response in the mesoscopic media, which are shown in the following section.

The resonant behavior of $\{F\}$ is clearly seen also in the distribution of the internal field in real space. The spatial distribution of the intensity of internal field $I_j(=|\mathcal{E}_j|^2)$ is shown in Fig. 2 for $N=10$, 52, 91, 401. In the case of $N=52$ (91), the spatial distribution at the lowest exciton energy is dominated by $|F_2|^2(|F_3|^2)$, which represents the spatial variation of induced polarization for $n=2(n=3)$ excitonic state. On the other hand, the spatial variation of the internal field for $N=10$ is hardly appreciable and its magnitude at the lowest exciton level is very small. For the large size ($N=401$), the amplitude of the internal field is much reduced by the damping and total reflection effect. Thus, we

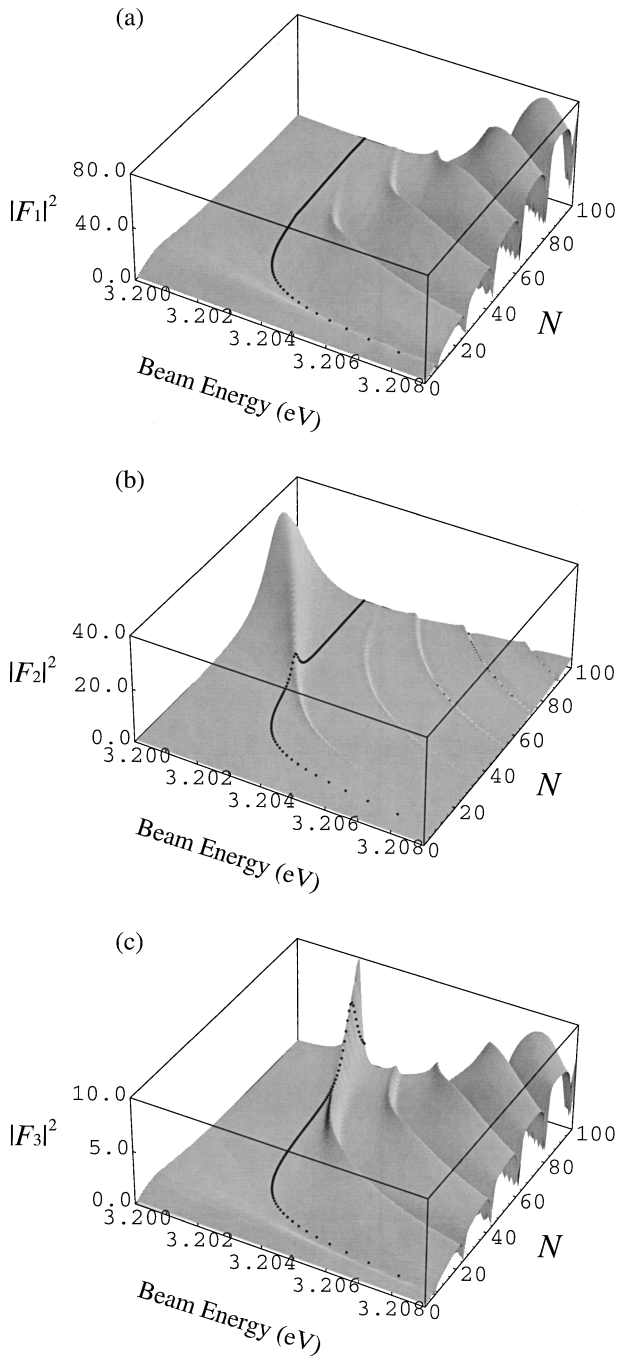

FIG. 1. $|F_n|^2$ (the strength of the component of the internal field related with the nth quantized exciton), as a function of beam energy and size N. (a), (b), and (c) are for $n=1$, 2, and 3, respectively. Dotted lines on the surface of $|F_n|^2$ indicate the values of $|F_n|^2$ at the lowest exciton level in each size. $\Gamma=0.06$ meV. The intensity of the incident beam is taken to be unity. The other parameter values are given in the text.

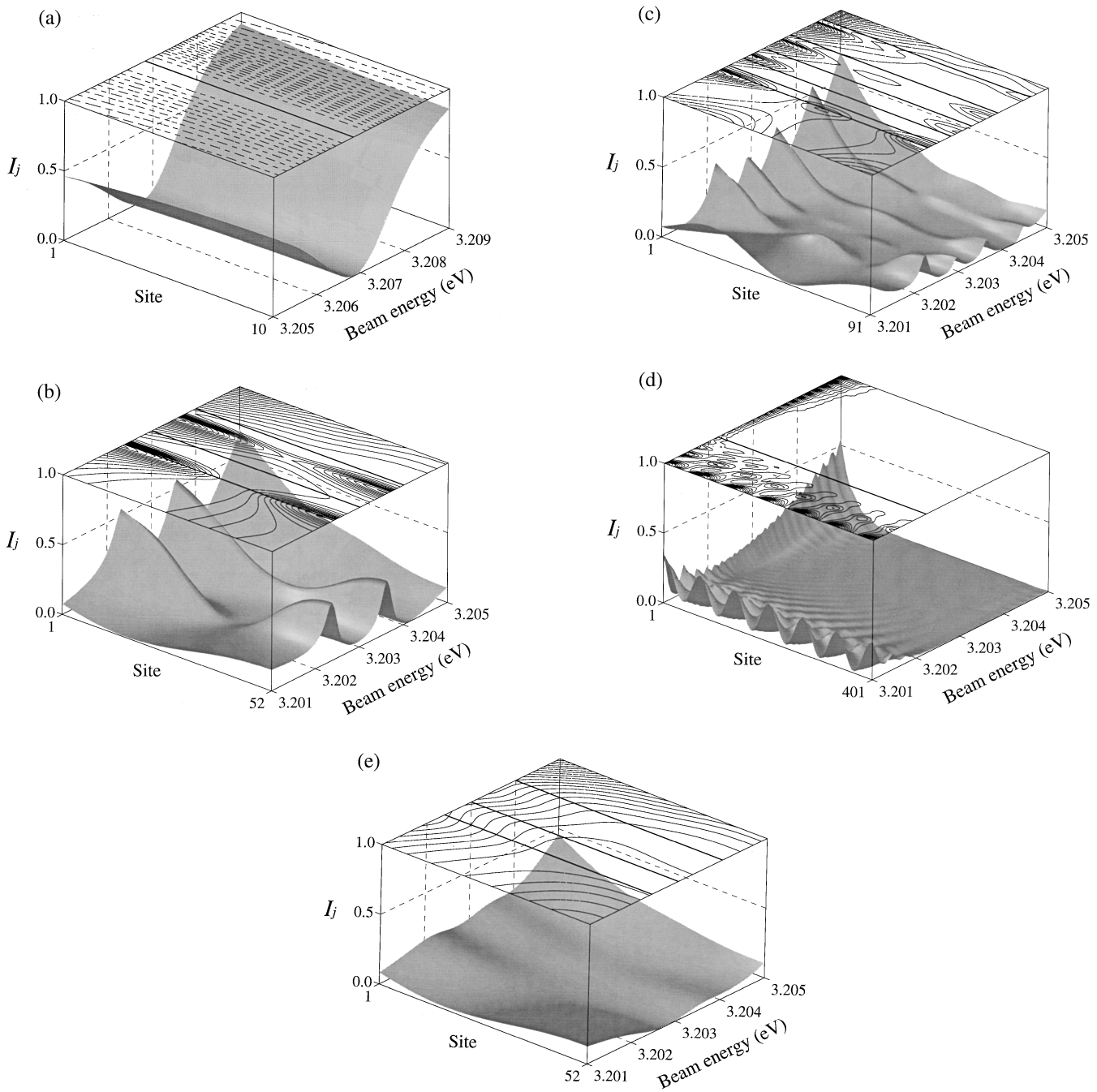

FIG. 2. The intensity of the internal field I_j as a function of discrete site j and beam energy for various sizes N. (a) $N=10$, (b) $N=52$, (c) $N=91$, and (d) $N=401$. The parameter values are the same as those in Fig. 1. (e) is the same as (b), but $\Gamma=0.6$ meV. Contour line of I_j and vertical lines indicating energy positions of one exciton are given on the top surface of each figure.

understand that the resonant enhancement of the internal field is a characteristic phenomenon in a limited range of mesoscopic size.

The extent of the enhancement of the internal field greatly depends on the value of transverse damping constant. Smaller damping causes a larger enhancement, while larger damping restrains the enhancement and the sharpness of the peaks of $|F|^2$ is reduced as the function of energy and size [Fig. 2(e)]. The smaller value that is taken here, 0.06 meV, is estimated from the analysis of an experimental result for a very good thin film of CuCl.[21]

As explained in Ref. 10, the resonant size enhancement of the internal field, which we show here, is explained in a general way in terms of the radiative correction, due to the retarded interaction among induced polarizations. The resonant energies of the response field, which we denote $\{\Omega_n\}$, are generally different from the corresponding material levels [the eigenvalue of unperturbed system, which we denote $E_1(n)$] by the radiative shift and width. This radiative shift increases as the system size increases (within LWA). In mesoscopic systems, the amount of the radiative shift can be larger than the separation of the neighboring size-quantized states that decreases as the size increases. Thus, if we fix the beam frequency ω to $E_1(m)$ and change the size, we find a

resonant enhancement of the internal field characteristic to the nth exciton state ($n \neq m$) at the size where $\mathrm{Re}(\Omega_n) = E_1(m)$ is realized.

The resonant enhancement of the internal field is equivalent to the known effect of polariton interference in the regime of linear response. In the nonlinear regime, however, the effect of nonlocal response has been very poorly studied, and therefore, we expect new types of nonlinear response for such a typically nonlocal condition as that for the resonant enhancement of internal field. Examples of such phenomena are presented in the next section.

III. NONLINEAR RESPONSE IN THE PRESENCE OF RESONANT ENHANCEMENT OF THE INTERNAL FIELD

To show the examples of the nonlinear response in the presence of the strong nonlocality, we calculate the pump-induced change in the probe spectra where the pump energy is in the excitonic resonant region. The probe beam scans the region near the transition energy between one-exciton states and bound two-exciton states.

In the size range we treat here, strong nonlocality appears through the resonant enhancement of internal field. In the previous work,[9] where the cancellation problem[7] was considered exactly, the size range was limited for numerical reasons. Here, we extend the range by relaxing the exact treatment, i.e., by omitting the less important terms in $\chi^{(3)}$. The choice of such terms is made by the detailed evaluation of the cancellation, as explained briefly in the next subsection. The model and the theory, which we outline below, are basically the same as in Ref. 9. (See Ref. 9 for more details.)

A. Model and theory

As a model system, we suppose a thin film consisting of a bundle of independent one-dimensional chains of size N confining Frenkel excitons, which lies perpendicular to the film surface, and both pump and probe beams are considered to be normal incidence. The unperturbed Hamiltonian is

$$\mathcal{H}_0 = \sum_{j=0}^{N+1} \varepsilon_0 a_j^\dagger a_j - b \sum_{j=1}^{N+1} (a_{j-1}^\dagger a_j + a_j^\dagger a_{j-1}) - \overline{\delta} \sum_{j=0}^{N} a_j^\dagger a_{j+1}^\dagger a_j a_{j+1}, \tag{9}$$

where $a_j^\dagger$ and a_j are the creation and annihilation operators of an exciton on the jth site, ε_0 the excitation energy of each site, b the transfer energy, and we introduce the virtual sites $j=0$ and $N+1$ on which the amplitude of exciton is supposed to be zero. The lattice constant of the chain is taken to be the unit of length. The third term, exciton-exciton interaction, is introduced to allow the bound two-exciton states. We treat δ as a free parameter for the above-mentioned purpose, though the binding energy of excitonic molecule (biexciton) will generally be very small in Frenkel-type excitons. The eigenvalues and eigenfunctions of one-exciton states are

$$E_1(n) = \varepsilon_0 - 2b\cos(K_n), \tag{10}$$

and

$$|K_n\rangle = \left(\frac{2}{N+1}\right)^{1/2} \sum_j \sin(K_n j) a_j^\dagger |0\rangle, \tag{11}$$

respectively. The allowed values of K_n are

$$K_n = \frac{n\pi}{N+1} \quad \{n = 1,2,\cdots,N\}. \tag{12}$$

To obtain two-exciton states, we expand them as

$$|\mu\rangle = \sum_{i<j} \overline{C_{i,j}^{(\mu)}} a_j^\dagger a_i^\dagger |0\rangle, \tag{13}$$

and calculate $\{\overline{C_{i,j}^{(\mu)}}\}$ and eigenvalues $\{\overline{E_\mu}\}$ numerically.

To calculate $\chi^{(3)}$ in nonlocal form, we use the usual perturbation expansion of density matrix as in Ref. 7, namely, we start with a standard expression of the third-order nonlinear polarization at site j and time t:

$$P_j^{(3)}(t) = \frac{(-i)^3}{v_0} \int_{-\infty}^{t} dt_1 \int_{-\infty}^{t_1} dt_2 \int_{-\infty}^{t_2} dt_3 \times \langle [[[P_j(t), \mathcal{H}'(t_1)], \mathcal{H}'(t_2)], \mathcal{H}'(t_3)] \rangle, \tag{14}$$

where the angular brackets mean a statistical average, v_0 is the volume of a unit cell, $\hbar$ is taken to be unity, $P(t)$ and $\mathcal{H}'$ are the interaction representations of the polarization operator and electron-radiation interaction, respectively,

$$P_j(t) = \exp(i\mathcal{H}_0 t) P_j \exp(-i\mathcal{H}_0 t), \tag{15}$$

$$\mathcal{H}'(t) = \exp(i\mathcal{H}_0 t) \left[-\sum_i \sum_s P_i \mathcal{E}_i(s) \exp(-i\omega_s t + \overline{\gamma t}) \right] \times \exp(-i\mathcal{H}_0 t), \tag{16}$$

$\overline{\gamma} = 0^+$ the factor for adiabatic switching of the electron-radiation interaction, and $\mathcal{E}_i(s)$ the amplitude of the electric field at site i with frequency ω_s. Inserting the matrix elements of site-dependent dipole density between the ground state and one-exciton states and between one- and two-exciton states, which are calculated with the known wave functions (11) and (13), we obtain $\chi^{(3)}$ in a nonlocal form for the arbitrary frequencies. In this calculation, we have introduced the phenomenological damping constants γ for the population decay and Γ for the phase decay in the usual way as in Ref. 22. Then, among all the terms of the nonlinear polarization, we pick up the contribution of the most (triply) resonant terms for the pump frequency ω_2 and probe frequency ω_1. The third-order polarization $P_j^{(3)}$ with frequency ω_1 is then written in the following form:

$$P_j^{(3)}(t)|_{[\text{tri. res.}]}=\frac{M^4}{v_0}\left(\frac{2}{N+1}\right)^{1/2}\sum_n \sin K_n j\Bigg[\sum_m |F_m^{(1)}|^2F_n^{(1)}G_0(K_n,K_m;\omega_1)$$
$$+\sum_m\sum_l\sum_k F_m^{(1)*}F_n^{(1)}F_k^{(1)}G_1(K_n,K_m,K_l,K_k;\omega_1)+\sum_m |F_m^{(2)}|^2F_n^{(1)}H_0(K_n,K_m;\omega_1,\omega_2)$$
$$+\sum_m\sum_l\sum_k F_m^{(2)*}F_k^{(2)}F_l^{(1)}H_1(K_n,K_m,K_l,K_k;\omega_1,\omega_2)+\sum_m F_m^{(2)*}F_n^{(2)}F_m^{(1)}\overline{H_0}(K_n,K_m;\omega_1,\omega_2)$$
$$+\sum_m\sum_l\sum_k F_m^{(2)*}F_l^{(2)}F_k^{(1)}\overline{H_1}(K_n,K_m,K_l,K_k;\omega_1,\omega_2)\Bigg]e^{-i\omega_1 t}, \tag{17}$$

where M is the transition dipole moment per site, G_0, G_1, H_0, H_1, H_0, and H_1 are the functions containing energy denominators, the explicit expressions of which are given in Appendix B in Ref. 9 with the slightly different notations. In the expression (17), we define the amplitudes $\{F\}$ as

$$F_n^{(p)}=\left(\frac{2}{N+1}\right)^{1/2}\sum_j \sin K_n j\,\mathcal{E}_j(p). \tag{18}$$

Note that the amplitudes $\{F\}$ are nothing but the expansion coefficients of the internal field in (7),[23] which is easily understood if we note that $\mathcal{E}_j(p)$ is obtained by reciprocal Fourier transformation of $F_n^{(p)}$. The polarization term in the Maxwell equations consists of the third-order term due to $\chi^{(3)}$ and the linear term. The latter is the sum of resonant term

$$P_j^{(1)}(t)=\frac{M^2}{v_0}\left(\frac{2}{N+1}\right)^{1/2}\sum_n \frac{\sin(K_n j)F_n^{(1)}}{E_1(n)-\omega_1-i\Gamma}e^{-i\omega_1 t}, \tag{19}$$

and background polarization. Regarding $\{F\}$ as given quantities, we can solve the Maxwell equations for $\{\mathcal{E}_j(p)\}$ in the form of cubic polynomials of $\{F\}$ with four arbitrary parameters (two for each of $\{\mathcal{E}_j(1)\}$ and $\{\mathcal{E}_j(2)\}$). Substitution of this solution into (18) leads to a set of cubic equations for $\{F^{(1)}\}$ and $\{F^{(2)}\}$, which, together with the Maxwell boundary conditions, can be solved uniquely for a given condition of incident field. (Because of the many unknowns $\{F_n^{(1)},F_m^{(2)}\}$, this calculation needs a large amount of computer work.) This unique solution fixes all the amplitudes of the internal and external fields.

In the computation of the nonlinear polarization in this work, we omit the terms containing the higher excitation energy than the relevant resonant energies, while we took account of all the levels in Ref. 9. For this treatment, a careful consideration of cancellation is necessary.[7] Namely, as system size increases, the cancellation occurs between the terms that contain ground state and two-exciton states in the second intermediate states in $\chi^{(3)}$, and a larger number of terms cancel for large system size. Because of this, the size linear enhancement of $\chi^{(3)}$ in the LWA regime tends to be suppressed and saturated to a size-independent constant value. Therefore, in the size region where the size enhancement is no longer linear, careless omission of the contributions of the higher levels would cause a large error. Since the extent of cancellation strongly depends on the material parameters, such as transfer energy and damping constant, we need to carefully examine case by case in omitting the contributions from the terms with higher excitation energies. We have performed such an examination by comparing the results of two different ways of computation for the same model as follows. In Ref. 7, we obtained the expression of $\chi^{(3)}$ of one-dimensional Frenkel excitons, with periodic boundary conditions, where the summation over the levels was analytically evaluated and the closed form of $\chi^{(3)}$ was obtained for an arbitrary size N. On the other hand, we can perform this summation partially in numerical calculation. By comparing the numerical results in LWA of these different treatments, we estimate the error arising from the omission of the higher levels for the relevant parameters. More details about this examination will be published elsewhere.

B. Results

Throughout this section, we use the values in (8) for the material parameters. Besides, we choose $\delta=195.0$ meV for the attractive energy of two excitons, and 7.2×10^4 V/m and 7.2×10^2 V/m for the amplitudes of the incident pump and probe beams, respectively. As for the damping constants, we use two sets, namely, the smaller set $(\gamma,\Gamma)=(0.02,0.06)$ meV and the larger set (0.2, 0.6) meV.

Since the signal intensity is functions of pump (ω_2) and probe (ω_1) frequencies and of sample size (N), we need to fix one of them to show the result in a 3D figure. In the following, we show two kinds of figures, either as functions of (ω_2,ω_1) or as functions of (ω_1,N). In the latter case, ω_2 is chosen at the energy of either $E_1(1)$ or the second lowest peak of the transmittance $T(\omega)$. As the nonlinear signal, we take the pump-induced change in the transmittance of the probe light. As for the case $\omega_2=E_1(1)$, we presented a brief report in Ref. 11, and discussed the change of the nonlinear signal with the size. In this paper, we give detailed discussions of the nonlinear processes of respective signals in all of the above cases. Before the detailed analysis of the signal that will be given in the next section, we glance through the overall behavior of the spectrum of each case.

Figure 3 shows the pump energy dependence of the nonlinear change in the transmittance spectrum of the probe beam $\delta T(\omega_1)$ for $N=50$. The pump energy covers the region where $|F_2|^2$ and $|F_3|^2$ take peak values in Fig. 1(b), 1(c), and the probe energy is near the transition energies

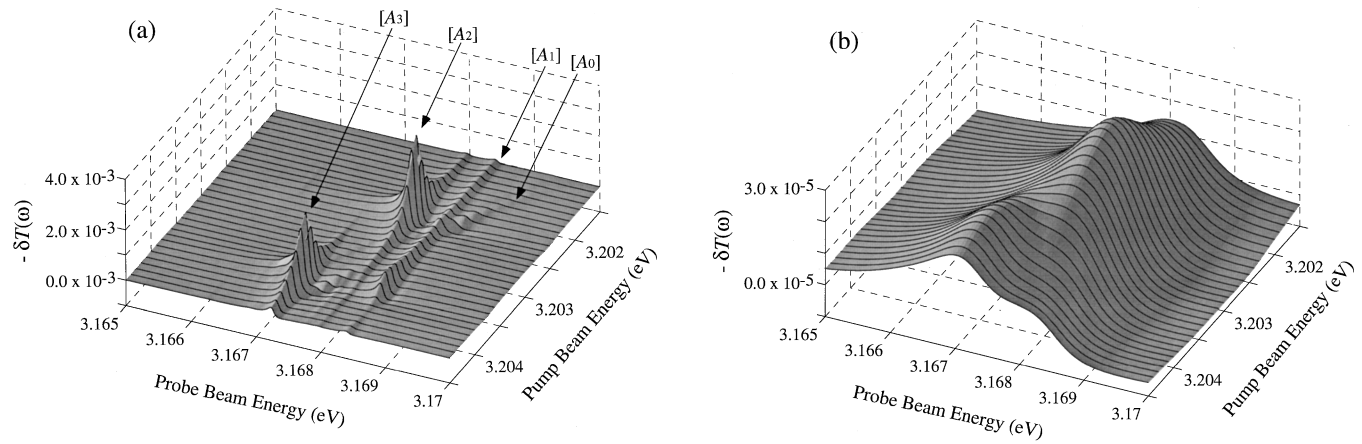

FIG. 3. Pump energy dependence of the negative value of the nonlinear change in the transmittance spectrum $-\delta T(\omega)$ of the probe beam for size $N=50$. (a) $(\gamma,\Gamma)=(0.02,0.06)$ meV, (b) $(\gamma,\Gamma)=(0.2,0.6)$ meV. The other parameters are given in the text. The meanings of $[A_n]$ $(n=0,$ 1, 2, and 3) are explained in the text.

between the (size-quantized) one-exciton and biexciton levels. Figures 3(a) and 3(b) are for the small and large damping, respectively. In Fig. 3(a), we can see three main structures near the constant values 3.1684 eV $[A_1]$, 3.1679 eV $[A_2]$, and 3.1672 eV $[A_3]$ of the probe beam. The peaks of these structures are due to the enhancement of F_n, namely, the transition by the probe beam between $E_1(n)\rightarrow E_n$ are strengthened by the enhancement of F_n, where E_n is nth biexciton level. Among them, the remarkable enhancement of $[A_2]$ and $[A_3]$, which reflect the pump energy dependence of $|F_2|^2$ and $|F_3|^2$ in Figs. 1(b), 1(c), should be noted. In addition, a small peak structure $[A_0]$ is due to the two-photon absorption satisfying $\omega_1+\omega_2=E_1$.

By comparing Figs. 3(a) with 3(b), we see that the magnitude of peaks and their sharpness is very dependent on the transverse damping constant Γ. (A change in γ affects only the magnitude of signals and does not change the sharpness.) The smaller value $\Gamma=0.06$ meV used in the present calculation corresponds to an experimental one for a very clean sample as mentioned in the previous section. The damping ten times as large as this value greatly reduces the magnitude of signals and its sharpness as seen in Fig. 3(b), and it becomes difficult to distinguish the peak structures of the respective nonlinear processes.

The effect of the resonant enhancement of internal field appears also in the size dependence of the pump-induced change of the probe spectrum in a characteristic way.[11] In Fig. 4, N dependence of $\delta T(\omega_1)$ is given for $\omega_2=E_1(1)$. Two distinct nonlinear signals and an additional small signal can be seen in Fig. 4(a). We denote them as $[B_0]$, $[B_1]$, and $[B_2]$ as shown in the figure. Their peak energies are $\omega_1=E_2-E_1(1)$ for $[B_0]$, $\omega_1=E_1-E_1(1)$ for $[B_1]$, and $\omega_1=E_2-E_1(2)$ for $[B_2]$, $[\omega_2=E_1(1)]$, at each size N. The small signal $[B_0]$, which is conspicuous around $N=50$, is due to the two-photon absorption where the total energy of pump and probe beam is identical to the eigenenergy of the second biexciton level E_2. The signal $[B_1]$, the size dependence of which is moderate, is due to two kinds of superimposed nonlinear processes, namely, pump-induced absorption by biexciton where the transition between $E_1(1)$ and E_1 occurs, and two-photon absorption, where the total energy of pump and probe beam is identical to $\overline{E_1}$. On the other hand, the strong size dependence of the signal $[B_2]$ is notable. The maximum of the peak very much exceeds that of signal $[B_1]$ around size $N=52$. The enhancement of this

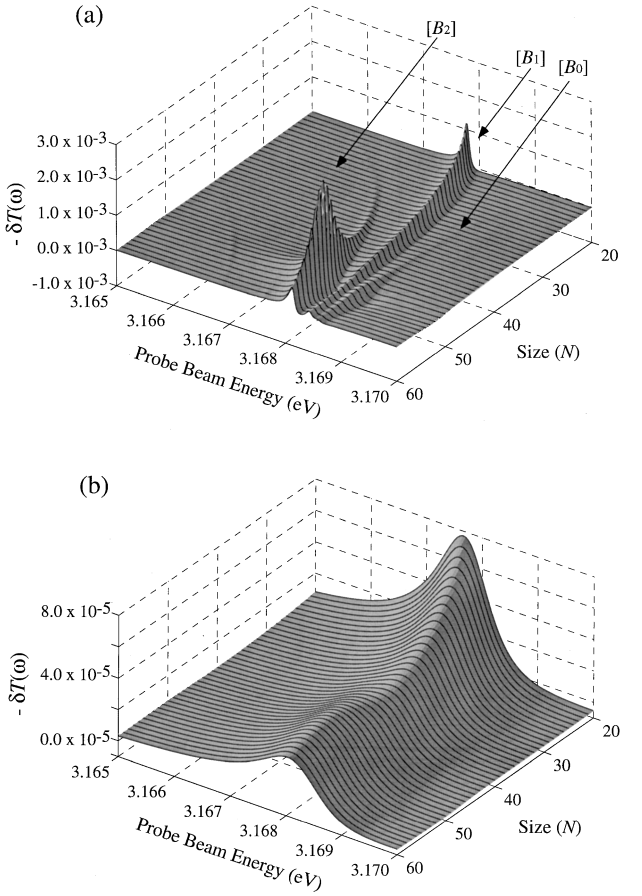

FIG. 4. Size dependence of the negative value of the nonlinear change in the transmittance spectrum $-\delta T(\omega)$ of the probe beam for the pump energy $\omega_2=E_1(1)$. $[E_1(n)$ is the eigenenergy of the nth one-exciton state.] (a) $(\gamma,\Gamma)=(0.02,0.06)$ meV, (b) $(\gamma,\Gamma)=(0.2,0.6)$ meV. The other parameters are given in the text. The meaning of $[B_n]$ $(n=0,$ 1, and 2) is explained in the text.

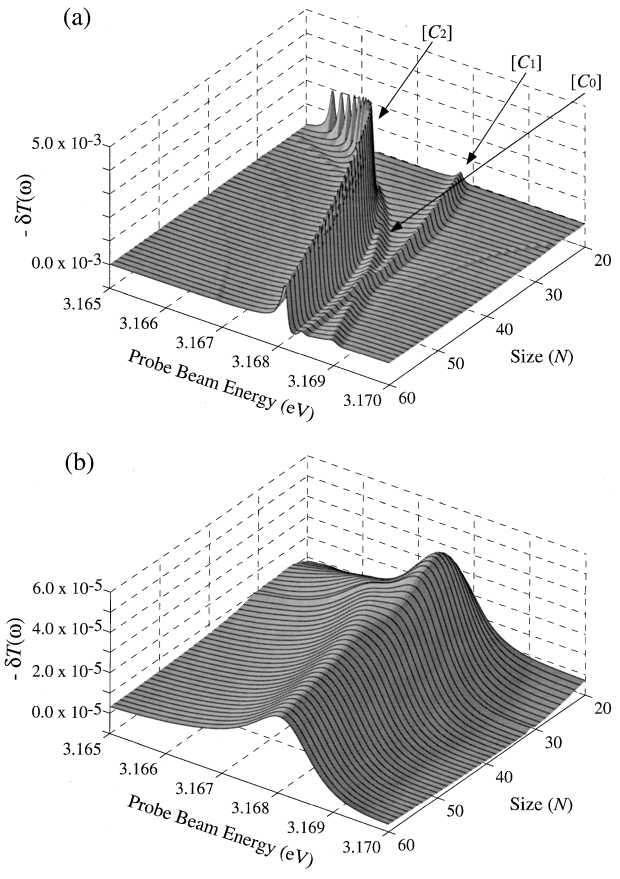

FIG. 5. Size dependence of the negative value of the nonlinear change in the transmittance spectrum $-\delta T(\omega)$ of the probe beam for the pump energy $\omega_2=\Omega_2$. (Ω_n is the nth resonant energy of the response field.) (a) $(\gamma,\Gamma)=(0.02,0.06)$ meV, (b) $(\gamma,\Gamma)=(0.2,0.6)$ meV. The other parameters are given in the text. The meaning of $[C_n]$ $(n=0,$ 1, and 2) are explained in the text.

nonlinear signal $[B_2]$ is due to the resonant size enhancement of $|F_2|^2$, and the size dependence of $[B_2]$ clearly reflects that of $|F_2|^2$ in Fig. 2 in Ref. 11. The result for the larger damping is shown in Fig. 4(b). The distinction between $[B_1]$ and $[B_2]$ is not very clear in this case and the size enhancement of $[B_2]$ cannot be seen.

From an experimental point of view, it is not easy to put ω_{pump} in resonance with $E_1(1)$, which is different from spectral resonance position because of its radiative shift. An easier way is to put ω_{pump} in resonance with a spectral resonance $\{\Omega_j\}$. We show the size dependence of the spectra corresponding to this case in Fig. 5. In the present model, however, the optical structure corresponding to the lowest exciton level is noticeable only for a very small size, and it disappears as the size increases [Fig. 1(a)]. Then the peak relevant to the second-exciton level takes the place of it, and this seemingly corresponds to the lowest resonant level. Thus, we tune the pump energy to the peak position of $|F_2|^2$ in each size that almost corresponds to the peak position (Ω_2) of transmittance in the size region of consideration. The three main peak structures in Fig. 5 are denoted as $[C_0]$, $[C_1]$, and $[C_2]$, as shown in the figure. Their peak energies are $\omega_1=\overline{E_1}-E_1(1)$ for $[C_0]$, $\omega_1=\overline{E_1}-\Omega_2$ for $[C_1]$, and $\omega_1=E_2-\Omega_2$, for $[C_2]$, $(\omega_2=\Omega_2)$, at each size

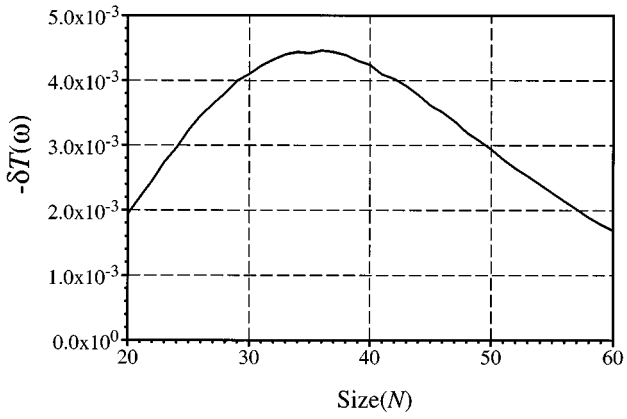

FIG. 6. Maximum value of peak $[C_2]$ in Fig. 5(a) for each size (N).

N. The signal $[C_0]$ and $[C_1]$ are due to the induced absorption from $E_1(1)$ to $\overline{E_1}$ and the two-photon absorption, $\omega_1+\omega_2=\overline{E_1}$, respectively. The signals of these two processes in Fig. 4 appear at the same energy position, and cannot be distinguished, because the pump energy (ω_2) is adjusted to $E_1(1)$ in that case. The large signal $[C_2]$ has essentially the same origin as $[B_2]$ in Fig. 4. The peak value of this signal generally increases with size, due to the increase in $|F_2|^2$ [along the ridge of Fig. 1(b)], but turns to decrease around $N=37$ (Fig. 6). The reason for the decrease is the off-resonance energy, $\Omega_2-E_1(2)$, in the denominator of $\chi^{(3)}$, which increases with the size. The result for the larger damping is shown in Fig. 5(b). The $[C_0]$ and $[C_1]$ cannot be distinguished and the signal $[C_2]$ is not very conspicuous as compared with the other signals.

IV. ANALYSIS OF NONLINEAR SPECTRA

To understand the nonlinear processes contributing the anomalous signals, due to the resonant enhancement of the internal field shown in the previous section, we need to see individual terms in $P^{(3)}$. In the present pump-probe spectroscopy, main contribution comes from the two terms in $P^{(3)}$ that contain two-exciton states. They appear from the fourth term in the square brackets of (17). The one is proportional to

$$\frac{|F_n^{(2)}|^2 F_m^{(1)}}{(\omega_1+i\Gamma-\widetilde{E}_{\mu n})(\omega_1+\omega_2+2i\Gamma-\overline{E_\mu})[\omega_2+i\Gamma-E_1(n)]}, \tag{20}$$

and the other is proportional to

$$\frac{-2\Gamma|F_n^{(2)}|^2 F_m^{(1)}}{(\omega_1+i\Gamma-\widetilde{E}_{\mu n})\gamma\{\Gamma^2+[E_1(n)-\omega_2]^2\}}, \tag{21}$$

where

$$\widetilde{E}_{\mu n}=\overline{E_\mu}-E_1(n) \tag{22}$$

(Ref. 24). The former is known as a term contributing to the two-photon absorption, where the sum frequency of two photons (ω_1 and ω_2 in the present case) becomes identical to the transition energy between the ground state and two-exciton

states, which contributes to signal $[A_0]$, $[B_0]$, $[C_0]$, and partly $[B_1]$. The latter represents the pump-induced transition from the one-exciton states $|K_n\rangle$ to the biexciton states $|\mu\rangle$ by a probe beam. For example, the case with $n=1$ is well known as pump-induced absorption where the transition from the lowest one-exciton state to the lowest biexciton state by the probe beam is induced by the pump beam.

The anomalous nonlinear signals, due to the resonant enhancement of the internal field shown in the previous section, are due to the latter process (21). To clarify the origin of the size and energy dependence of this process in the mesoscopic regime, we should note the two kinds of resonances contributing to the nonlinear response, i.e., the resonance with material levels that are the poles of the susceptibility of excitons, and the resonant enhancement of the response field. As discussed in Sec. II, the latter resonance brings about the enhancement of $\{F's\}$ in the numerators of (17). Both of them cause the enhancement of nonlinearity. In the condition of strong nonlocality, the effect of the resonant enhancement of $|F_n|^2$ much more often appears than those of the energy denominators of (21). Thus, the relative magnitudes of nonlinear signals strongly reflect those of $|F_n|^2$. For example, the pump-induced transitions between $E_1(n)$ and E_n for $n\neq 1$ appear as larger nonlinear signals than that for $n=1$ even when the pump energy is near $E_1(1)$, as seen in Fig. 3, 4, and 5. These signals would be very small if it were not for the resonant enhancement of $|F_n|^2$. It should be noted that the enhancement $|F_n|^2$ leads to the induced transition from $E_1(n)$ to E_n, not to $E_m(m\neq n)$. This is because the probe beam energy ω_1 is in the transparent region in the linear-response regime. This means the dominance of the uniform component in its spatial variation. The induced transition between $E_1(n)$ and E_m, due to such a uniform probe field, requires a quasi K-selection rule $K_n\cong K_m$ (Ref. 25).

The peak structures $[A_n]$ $(n=1, 2, 3)$ in Fig. 3 appear, regardless of the pump energy, at the probe energy positions $E_n-E_1(n)$ corresponding to the first factor in the denominator of (21). On the other hand, the strong resonant enhancement of $|F_n|^2$ appears in the pump energy dependencies of $[A_2]$ and $[A_3]$. The characteristic points are that $[A_2]$ and $[A_3]$ are remarkably strengthened for the size $N\sim 50$, with their peak values greatly exceeding that of $[A_1]$, and that the energy positions of the pump beam where the peak values of $[A_n]$ take the maximum are shifted from the material levels $E_1(n)$ by their radiative shifts. The shifted positions correspond to the resonant energy of the response field, where the resonant enhancement of $|F_n|^2$ occurs.

The appearance of the nonlocal effect in the nonlinear processes can be clearly seen also in the system size dependence. In Fig. 4, the signal $[B_1]$ contains both processes of terms (20) and (21), and both of them always go through a complete resonance with respect to all three factors in the denominators. The notable points are the strong enhancement of the signal $[B_2]$ at around $N=52$, and the fact that the maximum value of the peak is much larger than that of $[B_1]$, though the energy denominator of this process (21) does not enjoy the complete resonance. At this size $N=52$, pump beam that is tuned to $E_1(1)$ becomes equal to Ω_2, and this causes the enhancement of the spatial pattern relevant to $|K_2\rangle$ in the induced polarization and internal field, namely, it virtually excites the second one-exciton state selectively. Thus, the matrix element of $-\Sigma_j P_j\mathcal{E}_j$ between $E_1(2)$ and E_2 is enhanced, and a strong signal appears when the probe beam is resonant with $\tilde{E}_{22}$.

In the case of Fig. 5, the signal $[C_2]$, the origin of which is the same as that of $[B_2]$, stays much larger than any other signals at every size, because the pump energy follows the peak position of $|F_2|^2$. On the other hand, the difference between the pump energy and the material level $E_1(2)$ increases as size increases, and the resonance condition with respect to the third factor in the denominator of (21) becomes weak. Because of this effect, the peak value of $[C_2]$ turns to decrease for $N\geqslant 37$ through $|F_2|^2$ keeps increasing.

V. DISCUSSIONS

Based on a nonlocal response theory, we have discussed the resonant enhancement of internal field in mesoscopic systems, which is a remarkable manifestation of nonlocality, and showed an anomalous nonlinear response, due to this effect with a model calculation. Though there have been many arguments about the nonlinear-response focused on the resonant structure and the size dependence of $\chi^{(3)}$, the effect of resonant enhancement of response field on the nonlinear spectra has not been discussed so far. As we pointed out in the former papers,[8,11] the effect of the resonant enhancement of the internal field on the nonlinear response should not be neglected, and the nonlocal treatment is absolutely necessary to take account of this effect in the discussion of resonant nonlinear response. In this paper, we have performed explicit model calculations to show this point, and as a result, we have revealed different properties of the nonlinear response in the mesoscopic systems, namely, a strong resonant enhancement of the nonlinear signals and a peculiar size dependence of them.

For the clear understanding of the nonlinear response in the mesoscopic systems, we should recognize the following points: First, the motion of the resonant internal field is determined self-consistently with that of the induced polarization via a nonlocal relationship between them. Because of this, the internal field with a particular spatial pattern associated with an exciton state is enhanced at the resonant frequency of the response field, which is shifted from the exciton level, due to the retarded interaction depending on the system size. Second, the resonant behavior of the nonlinear response in the mesoscopic systems arises not only from the poles of nonlinear susceptibility that are the excitation energies of unperturbed material levels, but also from the resonant enhancement of the internal field. Namely, we should always consider the dependence of the two kinds of resonances on the system size and structure, to consistently understand the nonlinear response in the mesoscopic systems.

Considering the above points, we naturally understand the aspects due to strong nonlocality in the nonlinear response of mesoscopic systems. The characteristic point of this aspect is the strong enhancement of a particular nonlinear signal caused by the resonant enhancement of the internal field with a particular spatial pattern. This effect appears as peculiar energy and size dependencies of the nonlinear spectra arising from the size-dependent radiative shift, which can be cor-

rectly treated by, not local, but nonlocal response theory.

When we see the pump energy dependence of $[A_n]$ in Fig. 3(a), we find a strong enhancement of the nonlinear signal originating from the transition between the nth one-exciton state and nth biexciton state for $n=2$ and 3. It is shown that these signals become much larger than that for $n=1$ in the case of particular size ($N=50$). This pump energy dependence reflects the spectra $\{|F_n(\omega_2)|^2\}$ of the respective components of the internal field, and cannot be understood by the analysis of the nonlinear susceptibility alone. It is also notable that the pump energy giving the maximum value of $[A_n]$ is determined by the balance of the ω_2 dependencies of $|F_n|^2$ and the energy denominator of (21). This again indicates that we should consider the resonant structures of the nonlinear susceptibility and the resonance of the internal field as a whole to analyze the nonlinearity appearing in the response field.

From the fact that the third-order nonlinear polarization depends on the three variables ω_1, ω_2, and N, there are several different ways to describe the behavior of $P^{(3)}$ according to the choice of a fixed variable, as shown in Figs. 3, 4, and 5. If we fix the pump energy at a material level as in Fig. 4, we find a resonant size enhancement of the nonlinear signal $[B_2]$. This is because the radiative shift $E_1(2)-\Omega_2$ grows with the size and it exceeds the separations $E_1(2)-E_1(1)$ at a certain size ($N=52$). Namely, at a particular size, we have a situation that the transition between $E_1(2)$ and E_2 is strengthened by the resonant enhancement of the particular component of the internal field (F_2), with a spatial pattern relevant to $E_1(2)$, in spite of the fact that the pump beam is tuned to a lower level $E_1(1)$. A similar situation will generally occur, if we choose $\omega_2=E_1(n-1)$. Namely, at a particular size, F_n will be resonantly enhanced, which leads to the enhancement of the probe beam transition from $E_1(n)$ to E_n. On the other hand, if we fix the pump energy at a resonant pole of response field ($\omega_2=\Omega_2$) as in Fig. 5, the size variation of the enhanced signal roughly follows that of the peak value of the intensity of the enhanced internal field. Thus, the size dependence of $|F_n|^2$ gives the main contribution to that of the nonlinear response in this case.

The large nonlinear signals discussed in this paper are due to the simultaneous occurrence of the resonances with the poles of nonlinear susceptibility and response field. This may be regarded as double resonance in analogy with the case of ENDOR (electron nucleus double resonance).[26] The parameters (ω_1,ω_2,N) in our case would correspond to the microwave (ω_{mw}), radio wave frequencies (ω_{rf}) and g value(s) in ENDOR. Signal intensities are functions of these parameters, and along a given cross section in this parameter space (e.g., $N=$const or $g=$const), a doubly resonant condition for the remaining parameters $(\omega_1,\omega_2;\omega_{\mathrm{mw}},\omega_{\mathrm{rf}})$ leads to a large signal. In our previous papers,[10,11] we argued the condition for the cross section $\omega_2=E_1(1)$. In this case, we realize the resonant enhancement by choosing appropriate size (N) and energy (ω_1). Considering also that the enhancement of $|F_n|^2$ is a characteristic effect in the nonlocal system, we called the large signal(s) NIDORES (nonlocality-induced double resonance in energy and size). This is a remarkable manifestation of the nonlocal nature appearing in the nonlinear response, and we can expect this phenomenon to be a new source of a large nonlinearity.

In this paper, we compare the results for the small and large values of the transverse damping, because it is essentially related with the visibility of the nonlocal properties. As we see in Figs. 3, 4, and 5, we must be able to observe the effects of the resonant enhancement of the internal field on the nonlinear spectra clearly if the damping constant is as small as that of a 150-nm thin film of CuCl in Ref. 21, the damping constant of which was estimated to be about 0.06 meV in the analysis,[13] while it is difficult to observe them clearly if the damping constant is ten times larger than this value. The reason for this tendency is that the large damping reduces the coherence of the wave functions of quantized states and this causes the reduction of the nonlocality. Therefore, we should prepare clean samples with a small damping of exciton for the clear observation of the phenomena in consideration.

We have some problems in respect to restrictions of the present models for the linear and the nonlinear calculations. In the calculation of the linear response, we use the model of discrete lattice for the center-of-mass motion, and the internal degree of freedom of exciton is not considered. This model well reproduces the spectra of excitons with small Bohr radius. CuCl is a typical example of where the present model is applicable. For excitons with a large Bohr radius, the distortion of the wave function near the surfaces should be taken into account, which changes the quantization condition,[13] though the essence of the resonant enhancement of the internal field should not be different. In the nonlinear calculation, we use a special model, namely, the one-dimensional Frenkel excitons, where the transfer effect along the direction parallel to the surface is neglected. This treatment changes the level structure of the two-exciton states, which affects the cancellation problem.[7] Therefore, if we consider nonlinear processes involving scattering two-exciton states, a further examination of cancellation is necessary. However, if we consider nonlinear processes in the size region where the cancellation effect is not so serious, the present treatment of the cancellation problem mentioned in Sec. III is enough, and the behavior of the NIDORES effect is essentially unchanged by the use of the simplified model.

The resonant size enhancement of the internal field is expected to be a general effect in mesoscopic systems, regardless of the dimension of the confinement, but how it affects the enhancement of nonlinear signals should depend on material and specific processes to be considered. Therefore, the study of the resonant nonlinear response of the various types of confinements of the electronic systems, materials, and measurements in the presence of this effect would be necessary to obtain the comprehensive understanding of the nonlinear response of the nonlocal systems. Furthermore, such studies should also be interesting from an applicational viewpoint, because the resonant enhancement of internal field can be a guiding principle for finding large optical nonlinearity.

In the present stage, there has been no experimental report indicating the proposed phenomena in this paper, probably because the preparation of the size-controlled samples with good quality would not be easy. But the experimental verification of NIDORES is very much desired for the further

advance of this field, because it is one of the most characteristic manifestations of nonlocality in mesoscopic systems.

VI. SUMMARY

We have calculated the linear and nonlinear response of ultrathin film confining Frenkel excitons by means of a nonlocal method, and the following points are clarified. As a result of the self-consistent motion of internal field and induced polarization, which are related in a nonlocal way with each other, the internal field of a resonant light has a spatial distribution of a mesoscopic scale. At each resonance, shifted from an unperturbed exciton level by a radiative correction, a specific component of the internal field is enhanced. This effect is specific to nonlocal response, and cannot be derived from either the local response theory or a LWA of nonlocal theory.

The resonant enhancement of the internal field causes a different type of nonlinear response in mesoscopic systems. Namely, a nonlinear signal of a particular third-order process is much strengthened, due to the resonant enhancement of a particular component of the internal field at a resonant energy of a response field Ω_n. Because of it, the resonant structure of nonlinear spectra becomes quite different from those expected from the resonant structure of the nonlinear susceptibility in LWA alone. As an example, we have shown a case where the transition by probe beam between the nth one-exciton state $E_1(n)$ and nth biexciton state E_n is strengthened by the resonant enhancement of the internal field of the pump beam with a spatial pattern relevant to $E_1(n)$.

This large enhancement of the nonlinear signal can be regarded as due to the simultaneous occurrence of two resonances, one with sample size and another with material excitation energy. Thus, we propose to call this effect nonlocality-induced double resonance with energy and size as a source of large nonlinearity.

ACKNOWLEDGMENTS

The authors are grateful to Dr. Y. Ohfuti for his useful discussions. This work was supported in part by Grants-in-Aid for Scientific Research for Priority Areas ''Mutual quantum manipulation of radiation field and matter'' from the Ministry of Education, Science, Sports and Culture of Japan.

*Present address: Department of Material Physics, Faculty of Engineering Science, Osaka University, Toyonaka, Osaka 560, Japan.

[1] E. Hanamura, Solid State Commun. **62**, 465 (1987).
[2] E. Hanamura, Phys. Rev. B **37**, 1273 (1988).
[3] T. Takagahara, Phys. Rev. B **39**, 10 206 (1989).
[4] E. Hanamura, M. Kuwata-Gonokami, and H. Esaki, Solid State Commun. **73**, 551 (1990).
[5] L. Banyai, Y. Z. Hu, M. Lindberg, and S. W. Koch, Phys. Rev. B **37**, 8142 (1988).
[6] F. C. Spano and S. Mukamel, Phys. Rev. A **40**, 5783 (1989); Phys. Rev. Lett. **66**, 1197 (1991).
[7] H. Ishihara and K. Cho, Phys. Rev. B **42**, 1724 (1990).
[8] H. Ishihara and K. Cho, in *Proceedings of the International Symposium on Science and Technology of Mesoscopic Structure, Nara, 1991*, edited by S. Namba, C. Hamaguchi and T. Ando (Springer-Verlag, Berlin, 1992).
[9] H. Ishihara and K. Cho, Phys. Rev. B **48**, 7960 (1993).
[10] K. Cho, H. Ishihara, and Y. Ohfuti, Solid State Commun. **87**, 1105 (1993).
[11] H. Ishihara and K. Cho, Solid State Commun. **89**, 837 (1994).
[12] V. A. Kiselev, I. V. Makarenko, B. S. Razbirin, and I. N. Ural'tsev, Fiz. Tverd. Tela (Leningrad) **19**, 2348 (1977) [Sov. Phys. Solid State **19**, 1374 (1977)].
[13] K. Cho and M. Kawata, J. Phys. Soc. Jpn. **54**, 4431 (1985).
[14] A. D'ndrea and R. Del Sole, Phys. Rev. B **41**, 1413 (1990).
[15] K. Cho, A. D'ndrea, R. Del Sole, and H. Ishihara, J. Phys. Soc. Jpn. **59**, 1853 (1990).
[16] K. Cho, J. Phys. Soc. Jpn. **55**, 4113 (1986).
[17] K. Cho and H. Ishihara, J. Phys. Soc. Jpn. **59**, 754 (1990).
[18] H. Ishihara and K. Cho, Phys. Rev. B **41**, 1424 (1990).
[19] H. Ishihara and K. Cho (unpublished).
[20] K. Cho, Prog. Theor. Phys. Suppl. **106**, 225 (1991).
[21] T. Mita and N. Nagasawa, Solid State Commun. **44**, 1003 (1982).
[22] H. Ishihara and K. Cho, J. Nonlin. Opt. Phys. **1**, 287 (1991).
[23] Though the model in Sec. III is different from that of Sec. II in that the transfer in the lateral direction is (not) included in the latter (former), the expressions of F's and the internal fields in both models are the same as long as we consider the normal incidence.
[24] The expression (4.1) in Ref. 11 that corresponds to the expression (21) in this paper is mistyped and should be corrected to

$$\frac{-2\Gamma|F_n^{(2)}|^2F_m^{(1)}}{(\omega_1+i\Gamma-E_{\mu n})\gamma\{\Gamma^2+(E_n-\omega_2)^2\}}.$$

[25] N. Matsuura and K. Cho, J. Phys. Soc. Jpn. **64**, 651 (1995).
[26] G. Feher, Phys. Rev. **103**, 834 (1956).